J Toxicol Pathol 2013; 26: 175–186

Original Article

Thioacetamide-induced Hepatocellular Necrosis Is Attenuated in Diet-induced Obese Mice

Makoto Shirai[1*], Shingo Arakawa[1], Hiroaki Miida[1], Takuya Matsuyama[1], Junzo Kinoshita[1], Toshihiko Makino[1], Kiyonori Kai[1], and Munehiro Teranishi[1]

[1] Medicinal Safety Research Laboratories, Daiichi Sankyo Co., Ltd., 717 Horikoshi, Fukuroi, Shizuoka 437-0065, Japan

Abstract: To assess modification of thioacetamide-induced hepatotoxicity in mice fed a high-fat diet, male C57BL/6J mice were fed a normal rodent diet or a high-fat diet for 8 weeks and then treated once intraperitoneally with thioacetamide at 50 mg/kg body weight. At 24 and 48 hours after administration, massive centrilobular hepatocellular necrosis was observed in mice fed the normal rodent diet, while the necrosis was less severe in mice fed the high-fat diet. In contrast, severe swelling of hepatocytes was observed in mice fed the high-fat diet. In addition, mice fed the high-fat diet displayed more than a 4-fold higher number of BrdU-positive hepatocytes compared with mice fed the normal rodent diet at 48 hours after thioacetamide treatment. To clarify the mechanisms by which the hepatic necrosis was attenuated, we investigated exposure to thioacetamide and one of its metabolites, the expression of CYP2E1, which converts thioacetamide to reactive metabolites, and the content of glutathione S-transferases in the liver. However, the reduced hepatocellular necrosis noted in mice fed the high-fat diet could not be explained by the differences in exposure to thioacetamide or thioacetamide sulfoxide or by differences in the expression of drug-metabolizing enzymes. On the other hand, at 8 hours after thioacetamide administration, hepatic total glutathione in mice fed the high-fat diet was significantly lower than that in mice fed the normal diet. Hence, decreased hepatic glutathione amount is a candidate for the mechanism of the attenuated necrosis. In conclusion, this study revealed that thioacetamide-induced hepatic necrosis was attenuated in mice fed the high-fat diet. (DOI: 10.1293/tox.26.175; J Toxicol Pathol 2013; 26: 175–186)

Key words: obese, mouse, high-fat diet, thioacetamide, nonalcoholic fatty liver disease, liver

Introduction

Nonalcoholic fatty liver disease (NAFLD) is strongly related to obesity, a very common disease in developed countries[1]. NAFLD is present in up to one-third of adults in the USA[2] and is a well-known risk factor of inflammation, cirrhosis and cancer of the liver. NAFLD is considered to start by abnormal accumulation of triglycerides within hepatocytes. It has been reported that there are many abnormalities in the hepatocytes of patients with NAFLD, such as abnormalities in mitochondrial function[3, 4], drug-metabolizing enzyme expression[5–7] and impaired cell proliferation[8, 9]. Several animal models of NAFLD, such as an obesity-induced C57BL/6 mouse model fed a high-fat diet[8, 10], have been established. However, evaluations of drug-induced hepatotoxicity in animal models of NAFLD, which would be basic research in risk assessment for drug-induced hepatotoxicity in NAFLD patients, are limited.

Thioacetamide (TA) is a well-known hepatotoxicant that produces acute centrilobular necrosis in experimental animals by reactive metabolites[11]. CYP2E1 is a major drug-metabolizing enzyme that converts TA to thioacetamide sulfoxide (TASO) and TASO to the toxic reactive metabolite, thioacetamide disulfoxide ($TASO_2$)[12, 13]. Once the reactive metabolites are produced, they covalently bind to liver macromolecules[11]. Cellular oxidative stress is increased[14], and inflammation and DNA strand breaks occur[15].

In this study, we investigated TA-induced hepatic necrosis in mice fed a high-fat diet to confirm whether necrosis was modified.

Materials and Methods

Chemicals

TA was purchased from Wako Pure Chemical Industries, Ltd. (Osaka, Japan), and 5-bromo-2-deoxyuridine (BrdU) was purchased from Sigma-Aldrich Co. (Tokyo, Japan).

Animals and diets

Three-week-old male C57BL/6J mice were obtained from Charles River Laboratories Japan, Inc. (Yokohama,

Received: 3 December 2012, Accepted: 28 February 2013
*Corresponding author: M Shirai (e-mail: shirai.makoto.v7@daiichi-sankyo.co.jp)

Japan). They were housed under specific pathogen-free conditions in a controlled environment (21 to 25°C temperature, 45 to 65% relative humidity, twelve-hour dark-light cycle). Tap water was available *ad libitum*. Mice were fed a normal (conventional) rodent diet (CRF-1; Oriental Yeast Co., Ltd., Tokyo, Japan) or a high-fat diet containing 60 kcal% fat (High Fat Diet 32; Clea Japan, Inc., Tokyo, Japan) *ad libitum*. Body weight of the mice was measured every 2 weeks. This study was approved by the Ethics Review Committee for Animal Experimentation of Daiichi Sankyo Co., Ltd. and was conducted in compliance with the Law Concerning the Protection and Control of Animals (Japanese Law 105, October 1, 1973; revised on June 22, 2005).

Experimental design

After 8 weeks of feeding, mice fed the high-fat diet (HFD mice) or normal rodent diet (ND mice) were divided into four groups. Vehicle-HFD and vehicle-ND groups (n=4) were treated with saline once intraperitoneally and were necropsied at 24 hours after saline administration. TA-HFD and TA-ND groups were given TA (50 mg/kg body weight; dissolved with saline) once intraperitoneally and were necropsied at 8 (n=4), 24 (n=6) and 48 (n=6) hours after TA administration. The dose of 50 mg/kg was chosen based on an in-house preliminary study that showed hepatic necrosis in ND mice at 8 hours (minimal), 24 hours and 48 hours (severe) after treatment at this dose. The time points for necropsy were determined based on the preliminary study. Two hours before necropsy, all mice were given BrdU (100 mg/kg body weight; dissolved with saline) once intraperitoneally.

Collection of liver and blood samples for blood chemistry

At necropsy, all animals were euthanized by exsanguination under anesthesia. For the vehicle-treated mice only, exsanguination was performed after collecting the blood samples for blood chemistry from the inferior vena cava to investigate metabolic parameters. The livers of all animals were collected for histopathological examination and drug-metabolizing enzyme examination. For histopathology, the left lateral lobe and right and left medial lobes were trimmed and fixed in 10% neutral buffered formalin. The remaining portions of the livers were frozen in liquid nitrogen and stored at –80°C in a deep freezer for drug-metabolizing enzyme examination and hepatic glutathione analysis.

Blood chemistry

Plasma samples were prepared by centrifugation at 1,500 × g for 10 min. The concentrations of glucose (GLC), total cholesterol (TCHO) and triglyceride (TG) in the plasma were determined with an autoanalyzer (TBA-200FR, Toshiba Medical Systems Corporation, Tochigi, Japan).

Histopathological examination

The liver samples were fixed in neutral buffered formalin, routinely processed and embedded in paraffin and stained with hematoxylin and eosin (HE). Necrosis and swelling of hepatocytes were graded based on the histopathological characteristics of the specimens. TA-induced centrilobular necrosis and swelling of hepatocytes were judged to be very slight when they were observed only in hepatocytes adjacent to the central vein, and only in a few lobules. Hepatic necrosis was judged to be most severe when it involved several lobules [from zone 3 (centrilobular area) to zone 1 (periportal area)], and the necrotic tissue occupied most of the lobe. Even when it was most severe, swelling was limited to the lobules (from zone 3 to zone 2 (mid-zonal area)). Accordingly, TA-induced necrosis and swelling were graded as described below.

Centrilobular necrosis of hepatocytes

Grade 1: Centrilobular necrosis that reached zone 2 was observed in less than 5 lobules in the 3 lobes (the left lateral, right medial and left medial lobes).

Grade 2: Centrilobular necrosis that reached zone 2 was observed in 5 or more lobules, or centrilobular necrosis that reached zone 1 was observed in less than 5 lobules in the 3 lobes.

Grade 3: Centrilobular necrosis that reached zone 1 was observed in 5 or more lobules in the 3 lobes, and the necrotic area was less than 33% of 1 or more of the 3 lobes.

Grade 4: The necrotic area was 33% to 66% of 1 or more the 3 lobes.

Grade 5: The necrotic area was more than 66% of 1 or more of the 3 lobes.

Centrilobular swelling of hepatocytes

Grade 1: Centrilobular swelling was observed, but it was limited to the centrilobular area in the hepatic lobe (zone 3).

Grade 2: Centrilobular swelling that reached zone 2 was observed in less than 50% of lobules.

Grade 3: Centrilobular swelling that reached zone 2 was observed in 50% or more of lobules.

To evaluate lipid accumulation in hepatocytes, formalin-fixed liver samples of the vehicle-treated HFD mice were embedded in O.C.T. compound (Sakura Finetek Japan Co., Ltd., Tokyo, Japan) and stained with Oil Red O.

Immunohistochemistry

Immunohistochemistry was performed using a Dako EnVision system. Antigen retrieval for immunohistochemical staining was performed using an autoclave (121°C, 20 min). Mouse monoclonal antibody against BrdU (Immunotech, Fullerton, CA, USA, 1:50 dilution) and rabbit polyclonal antibody against CYP2E1 (Chemicon International, Temecula, CA, USA) were used as primary antibodies. The reaction products were visualized with 3,3'-diaminobenzidine tetrahydrochloride. Immunohistochemical study of BrdU and CYP2E1 was performed in all mice and vehicle-treated mice, respectively.

Five-bromo-2-deoxyuridine uptake index of hepatocytes

Microscopic fields were randomly selected in the periportal areas in a specimen of each animal. The periportal area was chosen because the centrilobular area showed necrosis. The number of BrdU-positive and BrdU-negative hepatocytes was counted (more than 3,000 hepatocytes) to investigate hepatocellular proliferation. The labeling index, expressed as the percentage of positive hepatocytes in the total number of hepatocytes, was calculated.

Terminal deoxynucleotidyl transferase-mediated dUTP-biotin nick end labeling assay

The terminal deoxynucleotidyl transferase-mediated dUTP-biotin nick end labeling (TUNEL) assay was performed on liver sections of all mice as previously described[16] to detect apoptotic hepatocytes. Briefly, the TUNEL method was performed using an ApopTag® Peroxidase In Situ Apoptosis Detection Kit (Chemicon International Inc., Temecula, CA, USA) according to the manufacturer's instructions.

Toxicokinetic analysis for thioacetamide and thioacetamide sulfoxide

Plasma samples for toxicokinetics were obtained from the tails of mice at 5, 15, 30, 60, 120 and 180 min after TA administration. Blood was collected three times from the same mouse at 5, 30 and 180 min or at 15, 60 and 120 min after administration. Twenty microliters of each plasma sample was mixed with 100 µl of methanol and centrifuged at 20,000 rpm for 5 min at 4°C. To determine the concentration of TA and thioacetamide sulfoxide (TASO), the supernatant was subjected to high-performance liquid chromatography (HPLC; Waters Corporation, Tokyo, Japan). The HPLC conditions for this analysis were as follows: the column was an L-column ODS (250 mm × 4.6 mm I.D., 5 µm, 12 nm, Chemicals Evaluation and Research Institute, Tokyo, Japan); the column temperature was 25°C; the mobile phase was 50 mM sodium sulfate, and 50 mM potassium phosphate buffer/acetonitrile (97/3, v/v); the flow rate was 0.85 ml/min; the injection volume was 10 µl; and the UV detector wavelength was 212 nm (for both TA and TASO).

Preparation of cytosol and microsomal fractions from mouse liver

The liver samples of vehicle-treated mice were homogenized in 1.15% KCl. The homogenate was then centrifuged at 9,000 × g at 4°C for 20 min, and the supernatant was centrifuged again at 105,000 × g at 4°C for 60 min. The resultant supernatant was used as the cytosolic fraction. The pellet was resuspended in 1.15% KCl containing 20% glycerol and used as the microsomal fraction.

Western blot analysis of drug-metabolizing enzymes

The cytosolic fraction was diluted to 2 mg/ml with 1.15% KCl and was used for the Western blot analysis for glutathione *S*-transferases (GSTs). The microsomal fraction was diluted to 2 mg/ml with 1.15% KCl containing 20% glycerol, and was used for the Western blot analysis for CYP2E1. The respective fraction was diluted to 2 mg/ml for GST analysis or 3 mg/ml for CYP2E1 analysis with Tris-SDS beta-mercaptoethanol sample loading buffer. The samples were heated at 95°C for 5 min and electrophoresed on 7.5% SDS-polyacrylamide gel (EASY-GEL, Funakoshi Co., Ltd., Tokyo, Japan) for CYP2E1 and 12.5% SDS-polyacrylamide gel (EASY-GEL) for GSTs, and they were then transferred electrophoretically onto Immobilon PVDF Transfer Membranes (Daiichi Pure Chemicals Co., Ltd, Tokyo, Japan) according to the methods of Burnette[17]. The membranes were incubated with primary antibody and streptavidin-horseradish peroxidase conjugate and then ECL Western blotting detection reagent (GE Healthcare Bio-Sciences KK, Tokyo, Japan). To detect the drug-metabolizing enzyme expression, antibodies against CYP2E1 (Chemicon International, Temecula, CA, USA), GSTA1, GSTA2, GSTA3, GSTA4, GSTP1 and GSTM1 (Proteintech Group, Inc., Chicago, IL, USA) were used.

Measurement of GST activities in cytosolic fraction

GST activity was measured using 1-chloro-2,4,-dinitrobenzene (CDNB), 1,2-dichloro-4-nitrobenzene (DCNB) or ethacrynic acid (EA) as a substrate (GST-CDNB, GST-DCNB and GST-EA activities, respectively) by the method of Habig *et al.*[18] using the cytosol fraction described above. CDNB, DCNB and EA were used as substrates for total GSTs, Mu-class GSTs and Pi-class GSTs, respectively. The protein concentrations of the microsome and cytosol fractions were determined according to the method of Lowry *et al.*, using bovine serum albumin as a standard[19].

Hepatic glutathione analysis

According to the manufacturer's instructions, total hepatic glutathione (GSH) and glutathione disulfide (GSSG) contents of vehicle- and TA-treated mice were measured using a Bioxytech GSH/GSSG-412 assay kit (OXIS International Inc., Foster City, CA, USA).

Statistical analysis

The results are expressed as the mean ± standard deviation (SD). The values of the mean and SD in each group were calculated with software (Microsoft Office Excel 2003; Microsoft, Redmond, WA). A parametric Dunnett's test (for comparison among 4 groups in the analysis of the labeling index of BrdU) or a combination of the F test and t-test (F-t test; for comparison between two groups) was performed to analyze the statistical differences in the mean values. For the F-t test, the homogeneity of variance was evaluated by an F test to determine whether the p-value was less than 0.25. After the homogeneity was determined, significant differences between the mean values were evaluated by a Student's t-test (for homogeneous data) or an Aspin-Welch t-test (for heterogeneous data).

Results

Effects of HFD on body weights, macroscopic findings and liver morphology

Body weights of HFD mice were significantly higher than those of ND mice after feeding for 2 weeks (i.e., at 5 weeks of age), and reached 1.39-fold higher than those of ND mice after feeding for 8 weeks (i.e., at 11 weeks of age, Fig. 1). After feeding for 8 weeks, vehicle-treated HFD mice had higher plasma concentrations of glucose and total cholesterol and lower plasma concentrations of triglycerides in comparison to the age-matched vehicle-treated ND mice (Table 1). At necropsy, a large amount of white adipose tissue was observed in the mesentery and around the kidneys in HFD mice (data not shown). The livers of HFD mice showed a yellowish discoloration. Microscopically, the hepatocellular cytoplasm of HFD mice was sparse, and microvesicular vacuoles were noted, mainly in zone 3 (Fig. 2-B). In samples stained with Oil Red O, the cytoplasm of the hepatocytes was stained red, thus confirming the hepatocellular fatty change (data not shown). These features indicated that feeding of a high-fat diet for 8 weeks was long enough to induce obesity and fatty liver in C57BL/6J male mice.

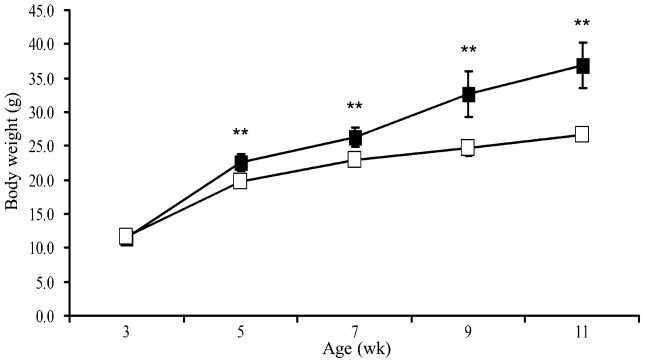

Fig. 1. Body weights in C57BL/6J male mice given the high-fat diet (HFD) or normal rodent diet (ND). The number of HFD mice was 34, 34, 30, 18 and 16 at 3, 5, 7, 9 and 11 weeks of age, respectively. The number of ND mice was 34, 34, 29, 16 and 16 at 3, 5, 7, 9 and 11 weeks of age, respectively. Black squares show the mean body weights of HFD mice, and white squares show those of ND mice. $^{**}p<0.01$ versus the weight of age-matched ND mice (Aspin-Welch t-test).

Histopathology of the liver in mice treated with TA

At 8 hours after TA administration, there was slight necrosis of hepatocytes in both HFD and ND mice. On the other hand, severe swelling of hepatocytes was noted from zone 3 to zone 1 in HFD mice, while slight swelling was observed only at zone 3 in ND mice (Fig. 2-C and 2-D, and Table 2). The swollen hepatocytes were finely stained, and had many microvesicles in the cytoplasm. Generally, the microvesicles were smaller than the lipid droplets observed in the hepatocytes of the vehicle-treated HFD mice. At 24 hours after TA dosing, 3 of 5 ND mice showed massive hepatocellular necrosis, and 1 of 5 of the animals was moribund before necropsy. On the other hand, the necrotic changes were less severe in HFD mice than in ND mice, as represented in the mean of the individual grades of necrosis (Fig. 2-E and 2-F, and Table 2). As was the case at 8 hours after administration, severe swelling of hepatocytes was noted only in HFD mice. This difference between HFD and ND mice was observed both at 24 hours and 48 hours after TA administration (Fig. 2-G and 2-H, and Table 2).

TUNEL assay of the liver in mice treated with TA

The TUNEL assay is an established and sensitive method for detection of apoptotic cells. Hence, TUNEL assays were performed to determine whether apoptosis occurred in swollen hepatocytes. At 8 hours after dosing, hepatocytes of HFD mice exhibited severe swelling as described above, but almost none of these hepatocytes exhibited TUNEL-positive nuclei or cytoplasm (Fig. 3-A). Swollen hepatocytes were still negative with the TUNEL assay at 24 and 48 hours after administration (Fig. 3-B and 3-C). On the other hand, nuclei and cytoplasm of hepatocytes determined to be necrotic cells with HE staining were TUNEL positive in both HFD and ND mice at 24 and 48 hours after administration (Fig. 3-B to 3-D).

BrdU immunohistochemistry of the liver in mice after TA administration

When immunohistochemistry was performed to detect BrdU uptake into hepatocellular nuclei, there was almost no labeling between 0 to 24 hours after TA administration, and no substantial difference between HFD and ND mice (Fig. 4). At 48 hours after dosing, HFD mice displayed a more than 4-fold higher number of BrdU-positive hepatocytes compared with ND mice (Fig. 4 and Fig. 5-A and 5-B).

Table 1. Effects of High-fat Diet Feeding on Blood Chemistry

Group	GLC (mg/dL)	TCHO (mg/dL)	TG (mg/dL)
ND	257.7 ± 37.54	92.7 ± 3.21	80.7 ± 18.56
HFD	358.3 ± 43.99 *	183.6 ± 6.65 **	25.8 ± 9.74 **

The number of mice was 4 in each type of diet. $^{*}p<0.05$ versus ND mice; $^{**}p<0.01$ versus ND mice (Student's t-test).

Hepatic CYP2E1 protein expression level

To evaluate the basal expression level of the hepatic TA metabolizing enzyme, immunohistochemistry and Western blot analysis for CYP2E1 were performed in vehicle-treated mice. Immunohistochemistry revealed that hepatocellular CYP2E1 was broadly expressed in HFD mice in comparison with ND mice (Fig. 6-A and B). In Western blot analysis, the liver of HFD mice expressed a 2-fold higher level of CYP2E1 in comparison with that of ND mice (Fig. 7-A and -B).

Hepatic protein expression levels and activities of GSTs

To assess basal capability for detoxification in the livers from ND and HFD mice, the hepatic GSTA1, GSTA2, GSTA3, GSTA4, GSTP1 and GSTM1 protein expression levels of vehicle-treated mice were investigated. Compared with that of the ND mice, the liver of the HFD mice expressed significantly lower levels of GSTs (Fig. 7-A and -B). This tendency was confirmed by measurement of the activities of GSTs. In HFD mice, the catalyzing potentials of GSTs against three substrates were significantly lower than in ND mice (Fig. 8).

Hepatic total GSH and GSSG content

Total hepatic GSH and GSSG were measured to evaluate the GSH-dependent hepatic protection state. Total GSH content was significantly lower in HFD mice at 8 hours after TA dosing compared with time point-matched TA-treated ND mice (Fig. 9-A). The GSH oxidative form, GSSG, was also investigated, but there was no statistically significant difference between the content of this form in HFD mice and ND mice (Fig. 9-B).

Toxicokinetics of TA and TASO

To assess exposure to TA and the first metabolite of TA, TASO, toxicokinetics analysis was performed. $TASO_2$ is a highly reactive metabolite and is not detectable, so toxicokinetics analysis of this metabolite was not performed. The TA concentration reached its peak at 5 minutes, and TASO did so at 60 minutes after TA dosing (Fig. 10). The plasma concentration profiles of TA and TASO showed no obvious difference between HFD and ND mice.

Discussion

HFD mice show hepatic steatosis, and have been commonly used as an NAFLD model. They have been reported to show physiological abnormalities, such as CYP2E1 up-regulation[4], decreased GSH[20] and impaired compensatory proliferation of hepatocytes[8, 9]. These abnormalities strongly suggested that HFD mice would be more sensitive to the hepatic necrosis induced by chemicals, especially by those that are harmfully metabolized by CYP2E1.

TA is such a hepatotoxicant. To exert hepatotoxicity, TA needs to be metabolized to TASO by CYP2E1, and then to a harmful metabolite, $TASO_2$[12, 21]. $TASO_2$ is highly reactive and causes hepatotoxicity through the formation of adducts to proteins[22], the generation of oxidative stress and lipid peroxidation[12, 14]. CYP2E1 is necessary for TA to cause hepatotoxicity. Pretreatment with a CYP2E1 inducer exacerbates TA hepatotoxicity[13], and TA is harmless in CYP2E1-null mice[12]. An adequate dose of TA given to rodents causes fulminant hepatic necrosis within 24 hours after a single administration[13, 23]. Hence, we expected that HFD mice would demonstrate more severe TA-induced hepatic necrosis than ND mice.

Contrary to our expectation, however, the necrotic hepatotoxicity of TA was attenuated in HFD mice. In ND mice, slight hepatocellular necrosis occurred at 8 hours after TA injection, the severity of the centrilobular necrosis reached its peak at 24 hours, and the necrosis faded a little at 48 hours. This transition was similar in HFD mice, but the necrotic changes were less severe. At 24 hours after TA administration, the livers from 3 out of 5 ND mice showed massive necrosis (grade 5), while none from the HFD mice

Table 2. Histopathological Scores of the Liver Lesions in HFD and ND Mice

Group	0 h (n=4)	8 h (n=4)	24 h (n=6) [a]	48 h (n=6)
ND				
Necrosis (#/grade) [c]	4, 0, 0, 0, 0, 0	3, 1, 0, 0, 0, 0	0, 0, 2, 0, 0, 3 [b]	0, 0, 3, 2, 1, 0
Mean score	0	0.3	3.8	2.7
Swelling (#/grade) [c]	4, 0, 0, 0	0, 4, 0, 0	2, 1, 2, 0 [b]	0, 4, 2, 0
Mean score	0	1.0	1.0	1.3
HFD				
Necrosis (#/grade) [c]	4, 0, 0, 0, 0, 0	2, 2, 0, 0, 0, 0	0, 0, 4, 1, 1, 0	0, 0, 5, 1, 0, 0
Mean score	0	0.5	2.5	2.2
Swelling (#/grade) [c]	4, 0, 0, 0	0, 0, 0, 4	0, 0, 0, 6	0, 0, 2, 4
Mean score	0	3.0	3.0	2.7

0, 8, 24, 48 h: vehicle control, and 8, 24 and 48 hr after TA administration, respectively. The numbers of ND mice were 4, 4, 5 and 6 at 0, 8, 24 and 48 hours after TA administration, respectively. The numbers of HFD mice were 4, 4, 6 and 6 at 0, 8, 24 and 48 hours after TA administration, respectively. Mean score is the mean of individual grades. a: The number of ND mice was 5 because of accidental death of one animal. b: One animal showing severe necrosis (grade 5) was moribund at 24 hours after TA administration. c: The numbers show the incidence of each grade (0 to 5 for necrosis and 0 to 3 for swelling), and the leftmost number represents grade 0.

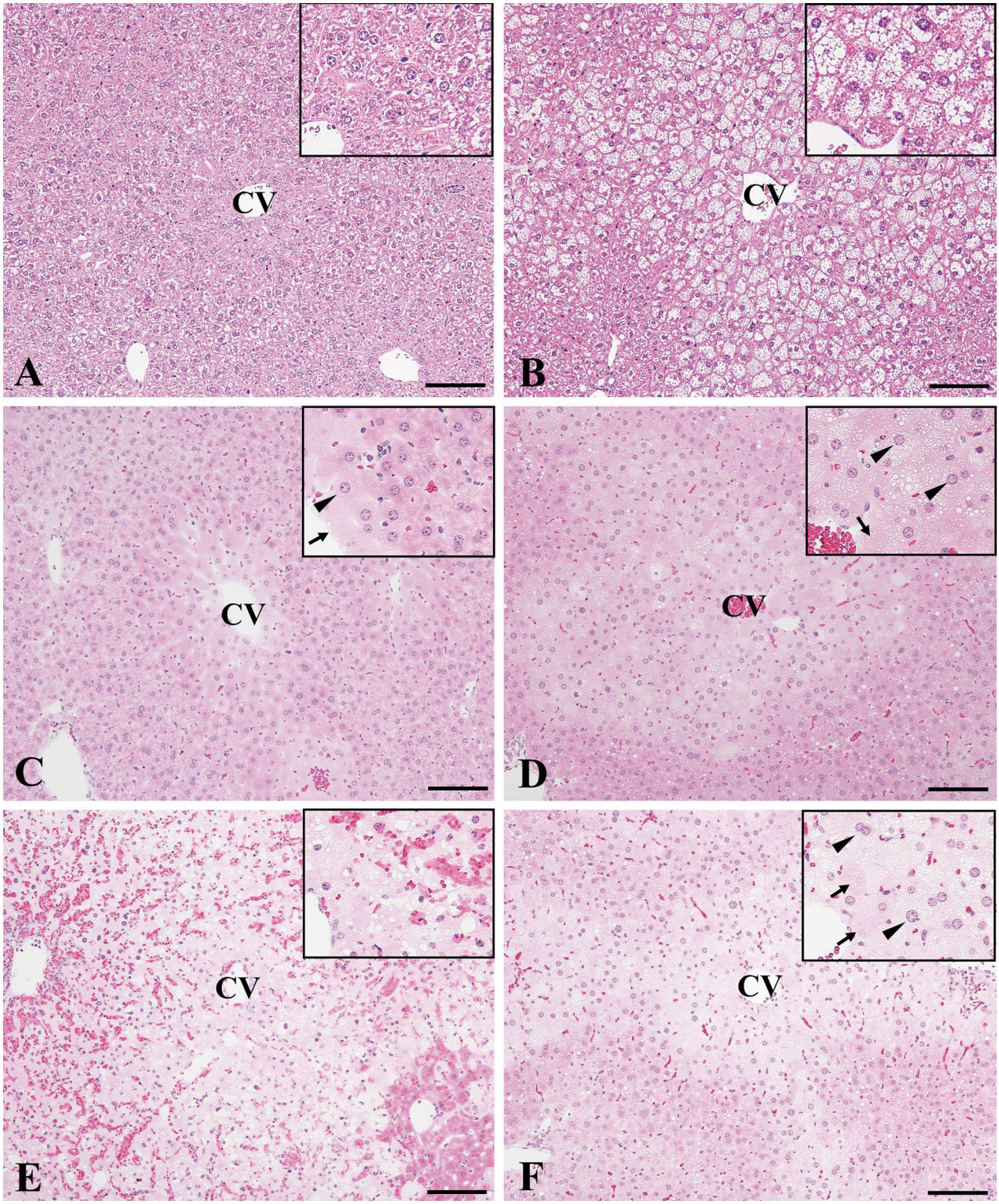

Fig. 2. Histopathological appearance of typical hepatic lesions in vehicle-treated mice and mice necropsied at 8, 24 and 48 hours after thioacetamide (TA) administration. A, C, E and G: The livers of mice fed the normal rodent diet at 0, 8, 24 and 48 hours after TA administration, respectively. B, D, F and H: The livers of mice fed the high-fat diet at 0, 8, 24 and 48 hours after TA administration, respectively. The detailed appearance around the central vein is shown in the inset in the right upper corner. Necrotic (arrow) and swollen (arrowhead) hepatocytes are shown. CV: central vein, HE stain, bar = 200 μm.

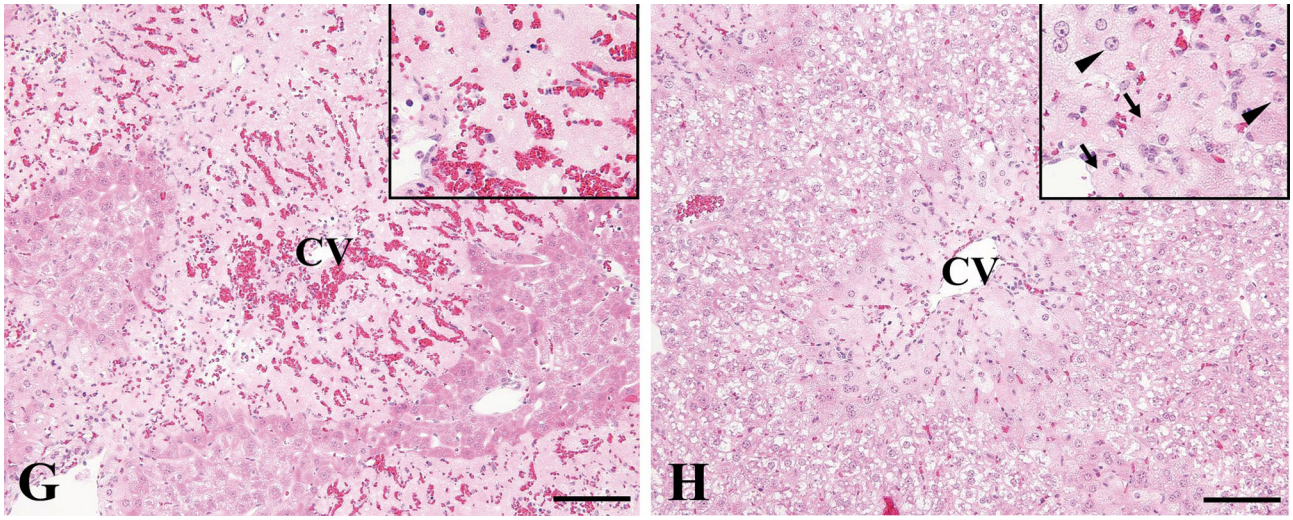

Fig. 2. Continued.

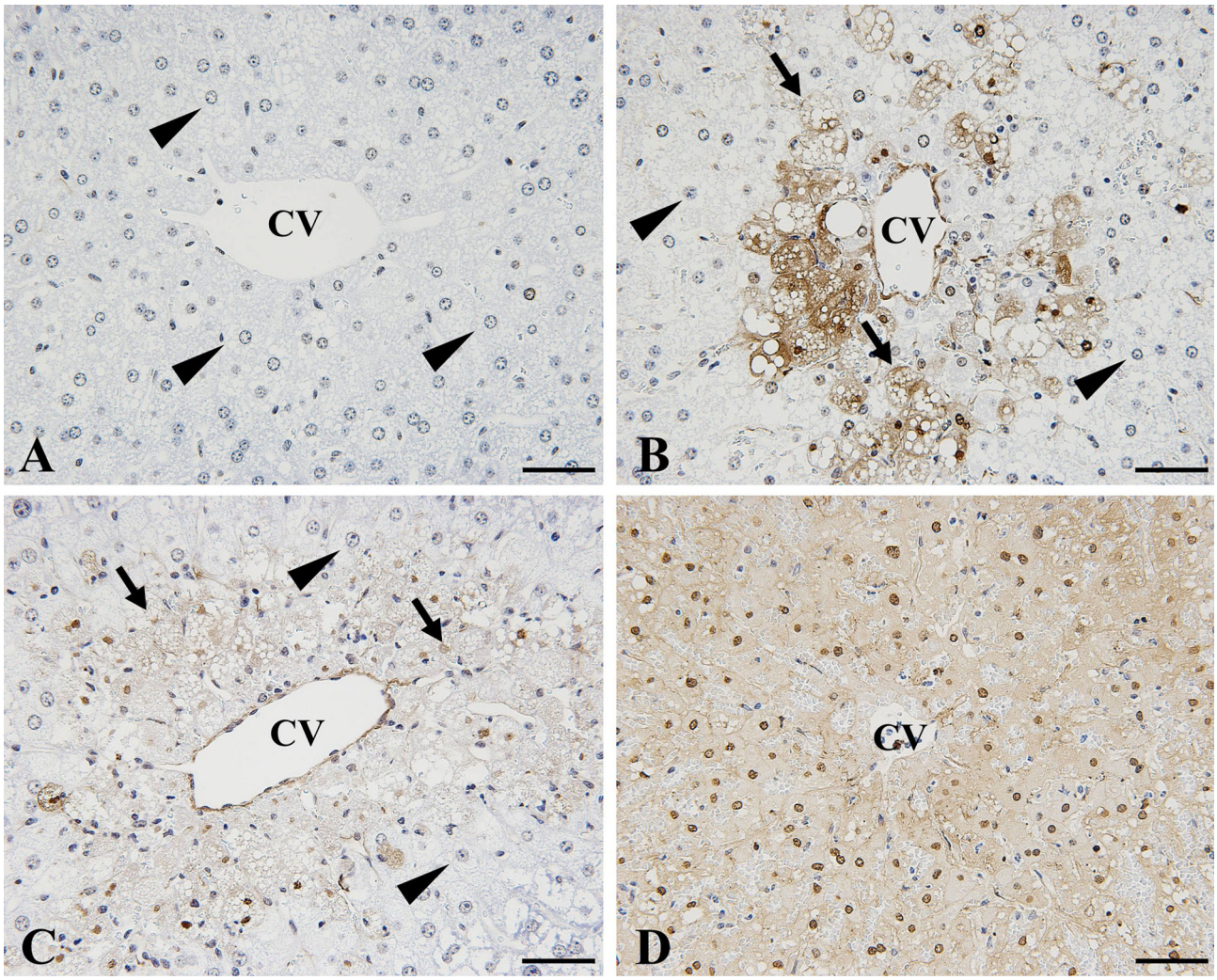

Fig. 3. TUNEL assay of the livers at 8, 24 and 48 hours after thioacetamide (TA) administration. A, B and C: The livers collected at 8, 24 and 48 hours after TA administration from mice fed the high-fat diet. D: The livers collected at 24 hours after TA administration from mice fed the normal rodent diet. Hepatocytes that were determined to be necrosis in the hematoxylin and eosin-stained specimens (arrow) were positively stained, while nuclei and cytoplasm of swollen hepatocytes (arrowhead) were negatively stained. CV: central vein, bar = 50 μm.

showed massive hepatic necrosis (Table 2). In addition, 1 of the ND mice became moribund at 24 hours after TA administration, probably because of massive necrosis, but none of the HFD mice showed abnormal clinical signs.

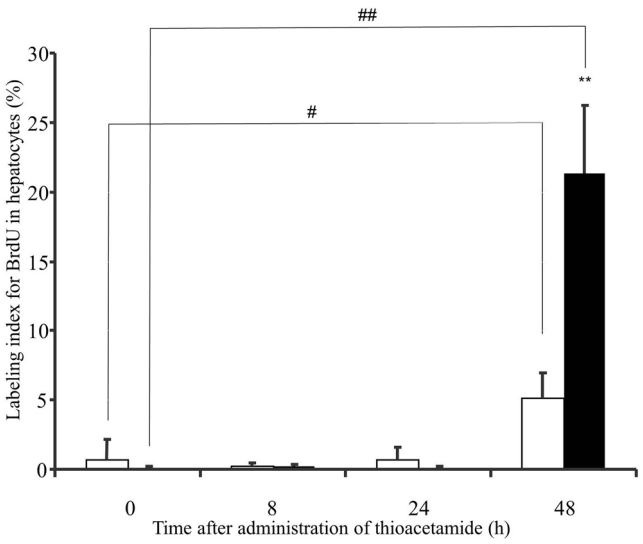

Fig. 4. Five-bromo-2-deoxyuridine (BrdU) labeling indices of hepatocytes of vehicle-treated mice (represented by 0 hour), and mice necropsied at 8, 24 and 48 hours after thioacetamide (TA) administration. The numbers of mice fed the high-fat diet (HFD) were 4, 4, 6, and 6 at 0, 8, 24 and 48 hours after TA administration, respectively. The numbers of mice fed the normal rodent diet (ND) were 4, 4, 5 and 6 at 0, 8, 24 and 48 hours after TA administration, respectively. Black columns: BrdU labeling indices in HFD mice. White columns: BrdU labeling indices in ND mice. $^{**}p<0.01$ versus the indices of administration time point-matched ND mice (Aspin-Welch t-test). $^{\#, \#\#}p<0.05$ and 0.01 versus the indices of the diet-matched control mice (0 h), respectively (Dunnett's test).

Instead of hepatic necrosis, swollen hepatocytes were broadly seen in HFD mice after TA administration. In addition to necrosis, apoptosis was reported to relate to TA-induced hepatotoxicity[24, 25]. When apoptosis occurs, the cells and/or cell fragments (apoptotic bodies) are often quickly phagocytized by adjacent macrophages or parenchymal cells, and apoptotic cells are therefore sometimes difficult to detect morphologically. The sensitivity for detecting apoptotic cells by the TUNEL assay has been reported to exceed that by morphological examination[26]. The TUNEL assay is a well-known method to detect DNA fragmentation of cells in the last phase of apoptosis, although this assay also detects necrotic hepatocytes as seen in this study[27]. To confirm whether apoptosis occurred frequently in swollen hepatocytes in HFD mice after TA dosing, a TUNEL assay was conducted. As a result, most of the swollen hepatocytes noted in HFD mice were almost negative. Therefore, the swollen hepatocytes were confirmed to be not apoptotic. We consider that swelling of the hepatocytes was probably a toxic change and was possibly caused by an osmotic disturbance and/or an abnormality of organelles. At present, the biological meaning of the swelling and the relationship between the swelling and the necrosis seen in hepatocytes are unknown. Further investigation, such as ultrastructural examination, is needed to clarify the changes within the swollen hepatocytes.

There are several possible mechanisms for the reduction in TA-induced hepatic necrosis in HFD mice. A different expression level of CYP2E1 is one of the possible mechanisms. As described above, TA is metabolized to TASO and then to a harmful metabolite, $TASO_2$, by CYP2E1[21]. In the present study, the hepatic expression of CYP2E1 was higher, and the area of the liver expressing CYP2E1 was broader in vehicle-treated HFD mice in comparison with

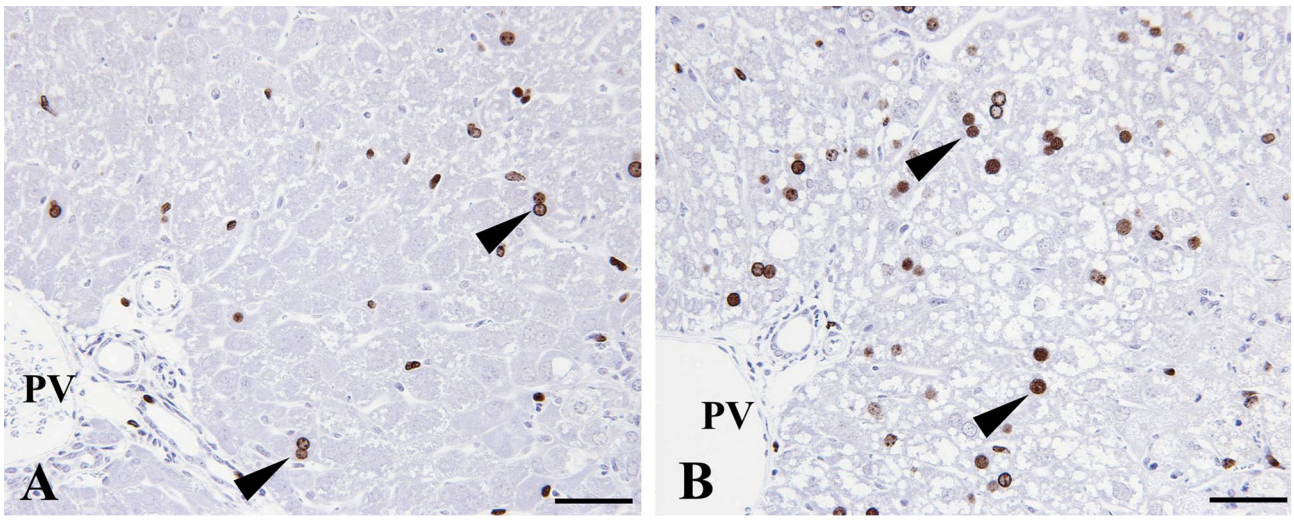

Fig. 5. Immunohistochemistry for 5-bromo-2-deoxyuridine in the livers from mice at 48 hours after thioacetamide administration. A: Liver from a mouse fed the normal rodent diet. B: Liver from a mouse fed the high-fat diet. Positively stained hepatocytes (arrowheads) are observed in the periportal area. PV: periportal vein, bar = 50 μm.

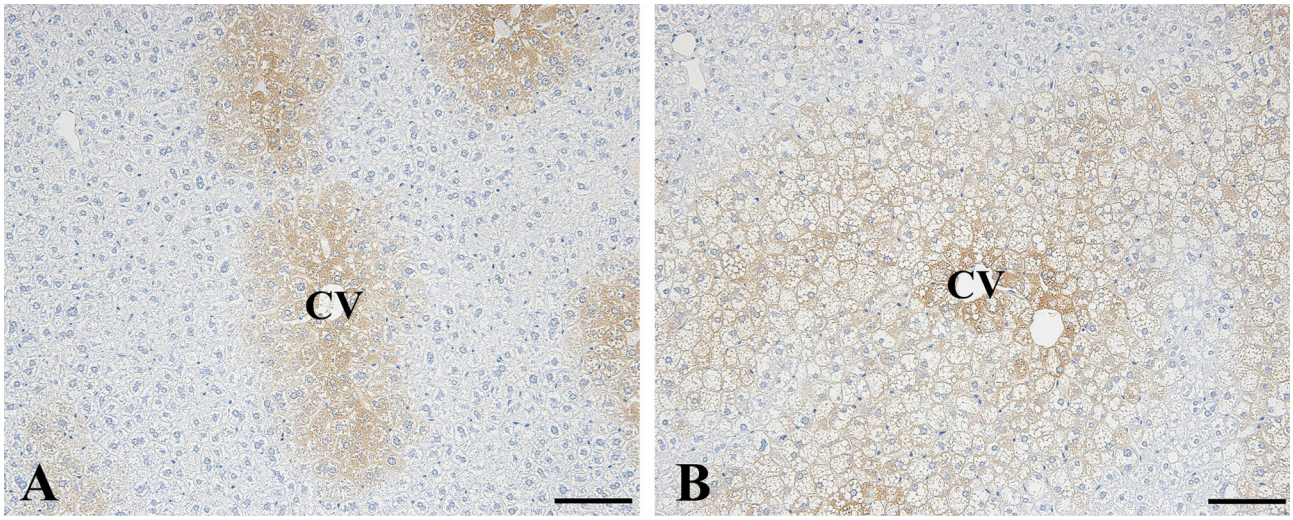

Fig. 6. Immunohistochemistry for CYP2E1 in the livers from the vehicle-treated mice. A: Liver from a vehicle-treated mouse fed the normal rodent diet. B: Liver from a vehicle-treated mouse fed the high-fat diet. CV: central vein, bar = 200 μm.

vehicle-treated ND mice. Therefore, the upregulation of hepatic CYP2E1 can likely be excluded as the mechanism of the attenuated TA-induced hepatocellular necrosis noted in HFD mice.

One of the other possible mechanisms for the lessened hepatic necrosis in TA-treated HFD mice could be a difference in exposure to TA or TASO. The HFD mice in this study showed a higher body weight gain, increased visceral fat and abnormalities in blood chemistry. The metabolic state changed with obesity. Therefore, abdominal absorption of TA, a water-soluble compound, and systemic distribution and excretion of TA and its pre-reactive metabolite, TASO, could be different between HFD mice and ND mice. In the present study, however, the plasma concentration profiles of TA and TASO showed no obvious difference between HFD and ND mice. Therefore, this indicates that the reduction in TA-induced hepatic necrosis in HFD mice is not attributable to reduced exposure.

Phase II drug-metabolizing enzymes are involved in conjugation reactions and are known to be engaged in detoxification, so they could be involved in a mechanism for the reduction of hepatocellular necrosis. In previous studies, it has been suggested that GSH protects against TA-induced hepatotoxicity[14, 28]; therefore, we focused on GSTs, which

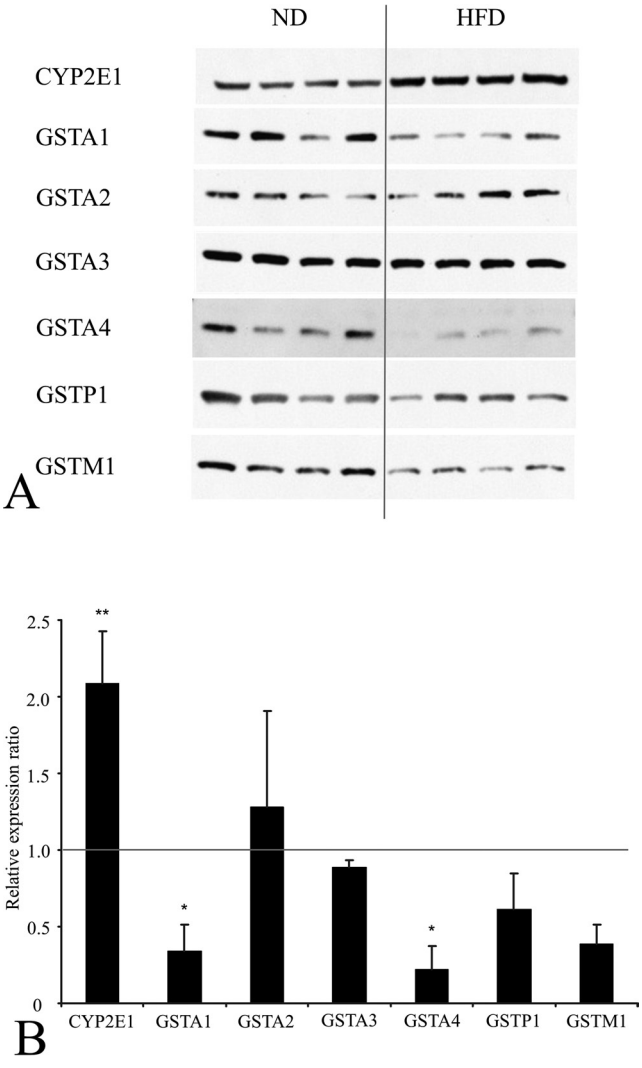

Fig. 7. Western blots of hepatic drug-metabolizing enzymes in the livers of vehicle-treated mice. The number of mice fed the high-fat diet (HFD) or normal rodent diet (ND) was 4. A: Western blots of CYP2E1, glutathione *S*-transferases (GST) A1, GSTA2, GSTA3, GSTA4, GSTP1 and GSTM1 of HFD mice and ND mice are shown. B: Expression of drug-metabolizing enzymes as quantified by densitometry is shown. Black columns show the relative expression ratios of HFD mice to ND mice. *, $^{**}p<0.05$ or $p<0.01$ versus the expression in mice fed the normal rodent diet, respectively (Aspin-Welch t-test).

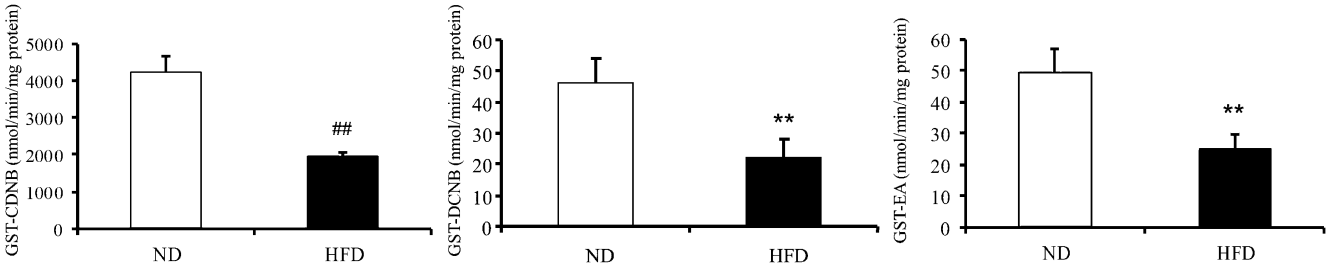

Fig. 8. Hepatic glutathione *S*-transferases (GST) activities toward 1-chloro-2,4,-dinitrobenzene (GST-CDNB), 1,2-dichloro-4-nitrobenzene (GST-DCNB) and ethacrynic acid (GST-EA) in the livers of vehicle-treated mice. The number of mice fed the high-fat diet (HFD) or normal rodent diet (ND) was 4. Black columns: Activities of HFD mice. White columns: Activities of ND mice. $^{**}p<0.01$ versus the activity of ND mice (Student's t-test). $^{\#\#}p<0.01$ versus the activity of ND mice (Aspin-Welch t-test).

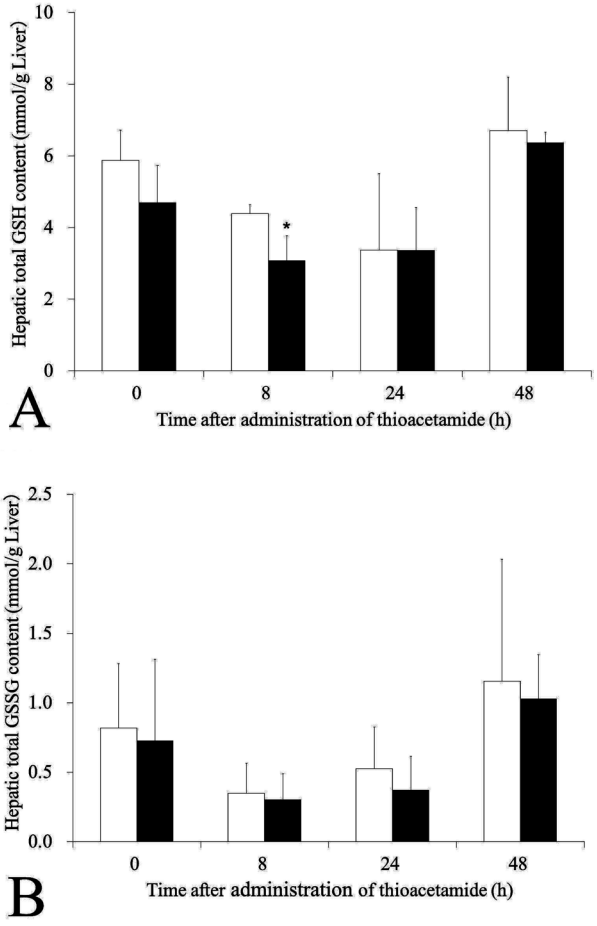

Fig. 9. Hepatic total glutathione (GSH) and glutathione disulfide (GSSG) content of vehicle-treated mice (represented by 0 hour) and mice necropsied at 8, 24 and 48 hours after thioacetamide (TA) administration. The numbers of mice fed the normal rodent diet (ND) were 4, 4, 5 and 6 at 0, 8, 24 and 48 hours after administration, respectively. The numbers of mice fed the high-fat diet (HFD) were 4, 4, 6 and 6 at 0, 8, 24 and 48 hours after administration, respectively. A: Hepatic total GSH content. Black columns: HFD mice. White columns: ND mice. B: Hepatic GSSG content. Black columns: HFD mice. White columns: ND mice. $^{*}p<0.05$ versus the content of administration time point-matched ND mice (Aspin-Welch t-test).

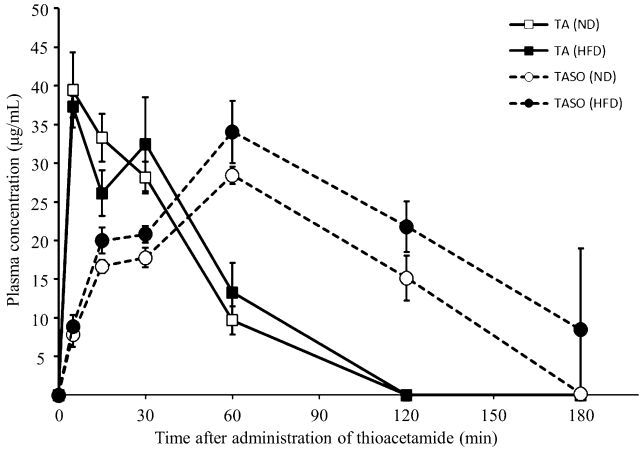

Fig. 10. Plasma concentrations of thioacetamide (TA) and thioacetamide sulfoxide (TASO) after TA administration. The number of mice fed the high-fat diet (HFD) or normal rodent diet (ND) was 4. Black squares: TA concentrations in HFD mice. White squares: TA concentrations in ND mice. Black circles: TASO concentrations in HFD mice. White circles: TASO concentrations in ND mice.

use GSH as a coenzyme. In the present study, the protein expression levels of many of the GSTs in the vehicle-treated group were lower in HFD mice compared with in ND mice. These results were supported by GST activity assays. The assays using 3 different substrates revealed that GST activity was significantly decreased in HFD mice. Hence, GSTs could not be involved in the mechanism of the reduction of the necrosis.

As mentioned above, GSH is believed to protect against TA-induced hepatotoxicity. It is an important coenzyme not only to conjugate metabolites but also to scavenge free radicals and suppress oxidative stress. GSH is converted to GSSG in the process of scavenging. GSSG is cytotoxic and drives apoptosis[29, 30], and Stankova *et al.* reported that the concentration of intracellular GSH decreased and that of extracellular GSSG increased after TA administration[28]. These previous reports suggest that GSH acts as a scavenger of free radicals that occur after TA dosing, and after scavenging, generated GSSG is exported to extracellular areas for cytoprotection. In the present study, total GSH

was significantly lower in HFD mice at 8 hours after dosing with TA compared with in ND mice at the same time after TA dosing, while there were no differences in GSSG levels. Taking these findings together, it is speculated that in HFD mice, increased GSH usage keeps hepatic oxidative stress low, and maintenance of a low concentration of GSSG lessens the hepatic damage from GSSG's cytotoxicity after TA dosing. We think that these changes in GSH/GSSG metabolism can partially explain why the TA-induced hepatic necrosis was less in HFD mice.

In the immunohistochemistry for BrdU, the BrdU-labeling index of hepatocytes did not differ from 0 to 24 hours after dosing with TA. Therefore, proliferative activity itself could not have caused the attenuated necrosis seen in HFD mice, at least within 24 hours after dosing. At 48 hours after dosing, marked hepatocellular proliferation was seen in HFD mice in comparison with ND mice. The proliferation of hepatocytes seen at 48 hours after dosing is considered to be compensation for the hepatocellular necrosis. The precise mechanisms responsible for this strong cell proliferation in HFD mice are unknown. However, we speculate that the strong proliferation was achieved, at least in part, because more intact hepatocytes remained in the liver of the HFD mice due to less necrosis. Compensatory cell proliferation is important for recovery; hence, more basic research is needed to clarify the pathophysiological condition of NAFLD.

There have been few reports regarding chemically-induced hepatotoxicity in obese animals, although such research is necessary for risk assessment of drug-induced hepatotoxicity in NAFLD patients. As for chemically-induced hepatotoxicity in high-fat diet-induced obese mice, only 2 reports have been published to date as far as we know. One report showed hepatotoxicity induced by acetaminophen[31], and the other showed hepatotoxicity induced by carbon tetrachloride[32]. But the results were inconsistent. The livers of HFD mice were less sensitive to the necrotic change induced by acetaminophen, while they were more sensitive to the necrosis induced by carbon tetrachloride. In addition, the regeneration after carbon tetrachloride-induced hepatic necrosis was blunted in HFD mice compared with that in ND mice[32]. We demonstrated that the hepatic necrosis induced by TA was reduced, so there is a possibility that TA- and acetaminophen-induced hepatic necrosis are attenuated in HFD mice by the same basic mechanisms. To advance basic research of risk assessment for drug-induced hepatotoxicity in NAFLD patients, further studies are needed to clarify what protects the liver of HFD mice from TA-induced hepatotoxicity.

In conclusion, we demonstrated that TA-induced hepatic necrosis was attenuated in HFD mice in comparison with ND mice. This is the first study to demonstrate that TA-associated hepatic necrosis is clearly reduced in the liver of HFD mice.

Acknowledgments: We would like to thank our colleagues for their extended care of the mice at our facility and Ms. Kimiko Hara, Shinobu Saito and Yoko Suzuki for their assistance with histopathological specimen preparation, Ms. Tomomi Sugiura for her assistance with toxicokinetics, and Ms. Masae Yagi for her assistance with Western blot analysis and measurement of GST activity.

References

1. Cohen JC, Horton JD, and Hobbs HH. Human fatty liver disease: old questions and new insights. Science. **332**: 1519–1523. 2011. [Medline] [CrossRef]
2. Farrell GC, and Larter CZ. Nonalcoholic fatty liver disease: from steatosis to cirrhosis. Hepatology. **43**: S99–S112. 2006. [Medline] [CrossRef]
3. Alberici LC, Vercesi AE, and Oliveira HC. Mitochondrial energy metabolism and redox responses to hypertriglyceridemia. J Bioenerg Biomembr. **43**: 19–23. 2011. [Medline] [CrossRef]
4. Mantena SK, Vaughn DP, Andringa KK, Eccleston HB, King AL, Abrams GA, Doeller JE, Kraus DW, Darley-Usmar VM, and Bailey SM. High fat diet induces dysregulation of hepatic oxygen gradients and mitochondrial function in vivo. Biochem J. **417**: 183–193. 2009. [Medline] [CrossRef]
5. Lee KY, Kim SJ, Cha YS, So JR, Park JS, Kang KS, and Chon TW. Effect of exercise on hepatic gene expression in an obese mouse model using cDNA microarrays. Obesity (Silver Spring). **14**: 1294–1302. 2006. [Medline] [CrossRef]
6. Merrell MD, and Cherrington NJ. Drug metabolism alterations in nonalcoholic fatty liver disease. Drug Metab Rev. **43**: 317–334. 2011. [Medline] [CrossRef]
7. Videla LA, Rodrigo R, Orellana M, Fernandez V, Tapia G, Quinones L, Varela N, Contreras J, Lazarte R, Csendes A, Rojas J, Maluenda F, Burdiles P, Diaz JC, Smok G, Thielemann L, and Poniachik J. Oxidative stress-related parameters in the liver of non-alcoholic fatty liver disease patients. Clin Sci (Lond). **106**: 261–268. 2004. [Medline] [CrossRef]
8. DeAngelis RA, Markiewski MM, Taub R, and Lambris JD. A high-fat diet impairs liver regeneration in C57BL/6 mice through overexpression of the NF-kappaB inhibitor, IkappaBalpha. Hepatology. **42**: 1148–1157. 2005. [Medline] [CrossRef]
9. Shirai M, Yamauchi H, Nakayama H, Doi K, and Uetsuka K. Expression of epidermal growth factor receptor protein in the liver of db/db mice after partial hepatectomy. Exp Toxicol Pathol. **59**: 157–162. 2007. [Medline] [CrossRef]
10. Clee SM, and Attie AD. The genetic landscape of type 2 diabetes in mice. Endocr Rev. **28**: 48–83. 2007. [Medline] [CrossRef]
11. Chilakapati J, Shankar K, Korrapati MC, Hill RA, and Mehendale HM. Saturation toxicokinetics of thioacetamide: role in initiation of liver injury. Drug Metab Dispos. **33**: 1877–1885. 2005. [Medline]
12. Kang JS, Wanibuchi H, Morimura K, Wongpoomchai R, Chusiri Y, Gonzalez FJ, and Fukushima S. Role of CYP2E1 in thioacetamide-induced mouse hepatotoxicity. Toxicol Appl Pharmacol. **228**: 295–300. 2008. [Medline] [CrossRef]
13. Wang T, Shankar K, Ronis MJ, and Mehendale HM. Potentiation of thioacetamide liver injury in diabetic rats is due

to induced CYP2E1. J Pharmacol Exp Ther. **294**: 473–479. 2000. [Medline]
14. Pallottini V, Martini C, Bassi AM, Romano P, Nanni G, and Trentalance A. Rat HMGCoA reductase activation in thioacetamide-induced liver injury is related to an increased reactive oxygen species content. J Hepatol. **44**: 368–374. 2006. [Medline] [CrossRef]
15. Yogalakshmi B, Viswanathan P, and Anuradha CV. Investigation of antioxidant, anti-inflammatory and DNA-protective properties of eugenol in thioacetamide-induced liver injury in rats. Toxicology. **268**: 204–212. 2010. [Medline] [CrossRef]
16. Ito K, Kiyosawa N, Kumagai K, Manabe S, Matsunuma N, and Yamoto T. Molecular mechanism investigation of cycloheximide-induced hepatocyte apoptosis in rat livers by morphological and microarray analysis. Toxicology. **219**: 175–186. 2006. [Medline] [CrossRef]
17. Burnette WN. "Western blotting": electrophoretic transfer of proteins from sodium dodecyl sulfate--polyacrylamide gels to unmodified nitrocellulose and radiographic detection with antibody and radioiodinated protein A. Anal Biochem. **112**: 195–203. 1981. [Medline] [CrossRef]
18. Habig WH, Pabst MJ, and Jakoby WB. Glutathione S-transferases. The first enzymatic step in mercapturic acid formation. J Biol Chem. **249**: 7130–7139. 1974. [Medline]
19. Lowry OH, Rosebrough NJ, Farr AL, and Randall RJ. Protein measurement with the Folin phenol reagent. J Biol Chem. **193**: 265–275. 1951. [Medline]
20. Lin CC, and Yin MC. Effects of cysteine-containing compounds on biosynthesis of triacylglycerol and cholesterol and anti-oxidative protection in liver from mice consuming a high-fat diet. Br J Nutr. **99**: 37–43. 2008. [Medline] [CrossRef]
21. Chilakapati J, Korrapati MC, Hill RA, Warbritton A, Latendresse JR, and Mehendale HM. Toxicokinetics and toxicity of thioacetamide sulfoxide: a metabolite of thioacetamide. Toxicology. **230**: 105–116. 2007. [Medline] [CrossRef]
22. Dyroff MC, and Neal RA. Studies of the mechanism of metabolism of thioacetamide s-oxide by rat liver microsomes. Mol Pharmacol. **23**: 219–227. 1983. [Medline]
23. Caballero ME, Berlanga J, Ramirez D, Lopez-Saura P, Gozalez R, Floyd DN, Marchbank T, and Playford RJ. Epidermal growth factor reduces multiorgan failure induced by thioacetamide. Gut. **48**: 34–40. 2001. [Medline] [CrossRef]
24. de David C, Rodrigues G, Bona S, Meurer L, Gonzalez-Gallego J, Tunon MJ, and Marroni NP. Role of quercetin in preventing thioacetamide-induced liver injury in rats. Toxicol Pathol. **39**: 949–957. 2011. [Medline] [CrossRef]
25. Ledda-Columbano GM, Coni P, Curto M, Giacomini L, Faa G, Oliverio S, Piacentini M, and Columbano A. Induction of two different modes of cell death, apoptosis and necrosis, in rat liver after a single dose of thioacetamide. Am J Pathol. **139**: 1099–1109. 1991. [Medline]
26. Gavrieli Y, Sherman Y, and Ben-Sasson SA. Identification of programmed cell death in situ via specific labeling of nuclear DNA fragmentation. J Cell Biol. **119**: 493–501. 1992. [Medline] [CrossRef]
27. Grasl-Kraupp B, Ruttkay-Nedecky B, Koudelka H, Bukowska K, Bursch W, and Schulte-Hermann R. In situ detection of fragmented DNA (TUNEL assay) fails to discriminate among apoptosis, necrosis, and autolytic cell death: a cautionary note. Hepatology. **21**: 1465–1468. 1995. [Medline]
28. Staňková P, Kucera O, Lotkova H, Rousar T, Endlicher R, and Cervinkova Z. The toxic effect of thioacetamide on rat liver in vitro. Toxicol In Vitro. **24**: 2097–2103. 2010. [Medline] [CrossRef]
29. Filomeni G, Rotilio G, and Ciriolo MR. Glutathione disulfide induces apoptosis in U937 cells by a redox-mediated p38 MAP kinase pathway. FASEB J. **17**: 64–66. 2003. [Medline]
30. Walther UI, Czermak A, Muckter H, Walther SC, and Fichtl B. Decreased GSSG reductase activity enhances cellular zinc toxicity in three human lung cell lines. Arch Toxicol. **77**: 131–137. 2003. [Medline]
31. Ito Y, Abril ER, Bethea NW, McCuskey MK, and McCuskey RS. Dietary steatotic liver attenuates acetaminophen hepatotoxicity in mice. Microcirculation. **13**: 19–27. 2006. [Medline] [CrossRef]
32. Allman M, Gaskin L, and Rivera CA. CCl4-induced hepatic injury in mice fed a Western diet is associated with blunted healing. J Gastroenterol Hepatol. **25**: 635–643. 2010. [Medline] [CrossRef]